Intermittent stimulation of the basal forebrain improves working memory in aged nonhuman primates.

Zhengyang Wang[1]*, Kendyl R Pennington[2] * Luca Debs[3], Sophia Chung[1], Janki Bava[4], Clement Garin[4], Fernando L. Vale[3], Sarah K Bick[4,6], Dario J Englot[4,6], Alvin V Terry[7], Christos Constantinidis[1,4,5]**, David T Blake[2]**

* These authors had equal contribution

** These authors equally share senior author responsibilities

1 Neuroscience Program, Vanderbilt University, Nashville, TN 37235

2 Dept Neuroscience and Regenerative Medicine, Medical College of Georgia, Augusta University, Augusta, GA

3 Dept Neurosurgery, Medical College of Georgia, Augusta University, Augusta, GA

4 Dept Biomedical Engineering, Vanderbilt University, Nashville, TN 37235

5 Dept. Ophthalmology and Visual Sciences, Vanderbilt University Medical Center, Nashville, TN 37232

6 Dept Neurosurgery, Vanderbilt University, Nashville TN

7 Dept Pharmacology/Toxicology, Medical College of Georgia, Augusta University, Augusta, GA

Abstract

Aging and some dementias feature parallel declines in the basal forebrain and cognitive capacity. Here, we tested the potential of one-hour daily intermittent basal forebrain stimulation to restore cognitive performance in aged male and female monkeys. Stimulation improved working memory in weeks, with performance remaining above study entry through the 15 month duration of the intervention. Effects persisted for at least 12 weeks after stimulation ceased. Parallel studies with a cholinesterase inhibitor did not produce lasting improvements in behavior. Brain stimulation led to immediate increases in tissue plasminogen activator levels in cerebrospinal fluid, and long-term increases in PET measures of glucose utilization. Intermittent basal forebrain stimulation thus triggers key components of neurotrophic signaling and leads to improved brain metabolism and better performance in working memory in senescent monkeys.

The cerebral cortex of mammals receives innervation from forebrain cholinergic neurons, which facilitate neurotransmission and maintain blood flow and neurotrophic tone in the neuropil[1,2]. The neurodegeneration in this pathway parallels declines in cognition that occur with aging and dementia and appears early in Alzheimer's disease[3–7]. The cholinergic basal forebrain region in the inferior aspect of the globus pallidus is the nucleus basalis of Meynert in primates, and it supplies cholinergic innervation to the cortical mantle[8]. If this region receives intermittent pulse train stimulation (e.g. for 20 s every minute) in young primates, humans, or mice, both acute and enduring executive function behavioral improvements can be measured[9–11]. However, continuous stimulation of the same region in animal models and humans with Alzheimer's, Lewy Body, or Parkinson's dementias is without enduring executive function improvement[12–14].

Limited duration pulse train stimulation of the basal forebrain increases cortical acetylcholine levels[1]. Pulse stimulation in the nervous system depolarizes membrane potentials in proportion to the second spatial gradient of the voltage field, often termed the activating function[15]. This function has a decline in efficacy at a distance close to the electrode, and this distance can be called the activating function radius. With suprathreshold stimulation, nearly all axons within the activating function radius will depolarize and generate action potentials[16]. With repetitive pulse train stimulation, these axons will recruit closely synaptically coupled neurons, and make the local circuit active. Our stimulation is applied to the nucleus basalis of Meyner to boost activity in its projection neurons.

The aged monkey represents an ideal model to investigate the potential of deep brain stimulation of nucleus basalis of Meynert to halt or reverse cognitive decline. The Rhesus macaque ages at roughly three times the rate of humans. The aged primate has declines in cognition analogous to those in humans[17]. Also like humans, beta-amyloid plaques form with age although the presence of neurofibrillary tangles composed of tau is more rare and appears shifted to a later age[18]. We investigated whether intermittent deep brain stimulation of the nucleus basalis of Meynert in senescent monkeys would halt or reverse cognitive decline.

Five Rhesus monkeys (2 male, 3 female) over the age of 25 (analogous to age >75 in humans) were implanted bilaterally with stimulating electrodes. The implantation target was the floor of the globus pallidus, in the medial-lateral center of the pallidal floor, and 2 mm posterior to the crossing of the globus pallidus by the anterior commissure, shown in Figure 1C and Figure S1. Implanted animals had been trained to perform a working memory task requiring them to remember a cue stimulus presented at the center of a screen and after a variable delay period, to select one of two test stimuli that matched the sample (Figure 1A). The behavior features a two-alternative forced choice procedure and used adaptive tracking to adjust the duration of the delay period. If the monkey chose correctly on three consecutive trials, the trial delay grew roughly 50% longer. Each error resulted in the delay shortening by 33%. This 3-up, 1-down adaptive tracking can be analyzed by averaging an even number of tracking reversals to converge on the 79% correct delay threshold[19] and allowed monkeys to perform using the same task parameters daily. After implantation and recovery, animals performed the working memory task daily, and received unilateral deep brain stimulation consisting of a 60 Hz train of pulses for 20 seconds interspersed with 40 second periods without pulses, for one hour daily. A pulse amplitude of 0.5 mA was chosen to produce an estimated activating function radius of 700 μm. We were particularly interested in the potential usefulness of the deep brain stimulation as a means of improving

cognitive function even when not specifically synchronized with task execution, therefore we delivered stimulation during the task on half the days, and after the task on half the days.

Over the three-month period after the initiation of stimulation, the animals' delay thresholds increased (Figure 1B, D). During the stimulation period, the monkeys were correct more often, and tracked to longer intervals. Their changes in threshold are shown in Figure 1D for sessions when the task was performed daily prior to stimulation. A repeated measures ANOVA on this data was significant ($F(1,4)=73.1$, $p<0.002$. Posthoc testing indicated that each of the five monkeys significantly increased their delay threshold as a result of stimulation ($p<0.05$ Tukey HSD post hoc for each pair).

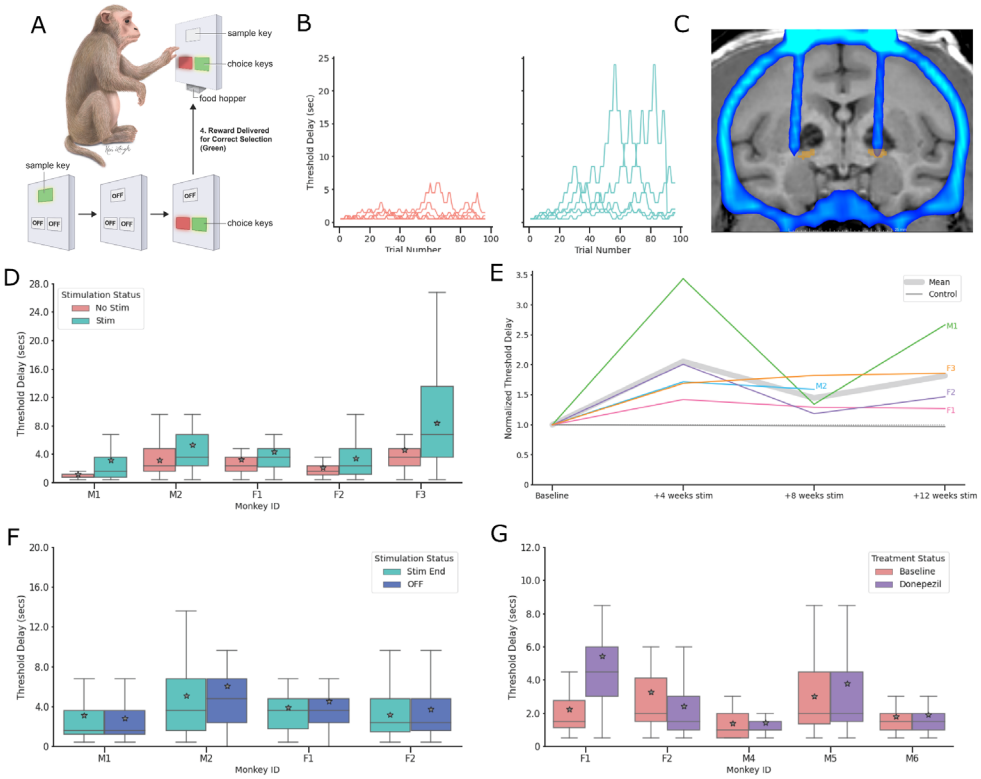

Figure 1. A. Monkey task. The monkey touches the cue on the touchscreen. The squares darken for the delay period. Then, a match and a distractor appear in the lower squares for the choice. B. Adaptive tracks for monkey performance for one animal before stimulation onset, and in the last four days of stimulation in the first 12 weeks. C. Target electrode placement from CT superimposed on a coronal MRI. The target was the mediolateral center of the globus pallidus, in the floor of the globus pallidus, 2 mm posterior to the crossing of the pallidus by the anterior commissure D. Single animal changes in working memory threshold in the first 8-12 weeks of stimulation. Five animals had electrodes in the target region and were stimulated unilaterally for one hour per day. E. Normalized individual changes in threshold each four weeks, and group average (thick gray line), for the same five animals as in D. F. Threshold changes compared across the last four weeks of stimulation for four of the animals in D compared to the next 12 weeks after ceasing stimulation. The four animals at the Augusta location were included. H. Changes caused by donepezil treatment for 12 weeks in five animals not receiving stimulation.

To assess the time course of changes, we grouped the normalized monkey tracking reversals in four week periods after the initiation of stimulation. An ANOVA on this timed data found significant a significant effect of time interval on the group means across the four week periods ($F(1,3)=55.3$, $p<10^{-4}$), and the 8-12 week period was highest, and significantly higher than the 4-8 week period in the posthoc test (Tukey HSD test $p<0.01$), but not the 0-4 week period.

In the three months after the initial stimulation period, four of the monkeys were continued in testing without further stimulation. A repeated measures ANOVA on this data was not significant ($F(1,3)=6.32$, $p<0.09$), suggesting no precipitous decline in performance after stimulation was halted (Figure 1F).

To determine the longevity of the effect, the animals that had received deep brain stimulation were given more stimulation, either unilateral or in some cases bilateral (see Figure S4), and their working memory thresholds tracked, for months after onset. All five animals retained supranormal working memory thresholds throughout

study, over time periods as long as 15 months after implantation, as shown in Figure 2. Aggregate monkey reversal data were significantly above 1 at all time points (t values 36.4, 23.2, 15.7, and 7.6 at 6, 9, 12, and 15 months, all $p<10^{-6}$). The three month data in Figure 2 are the same as those shown in Figure 1D.

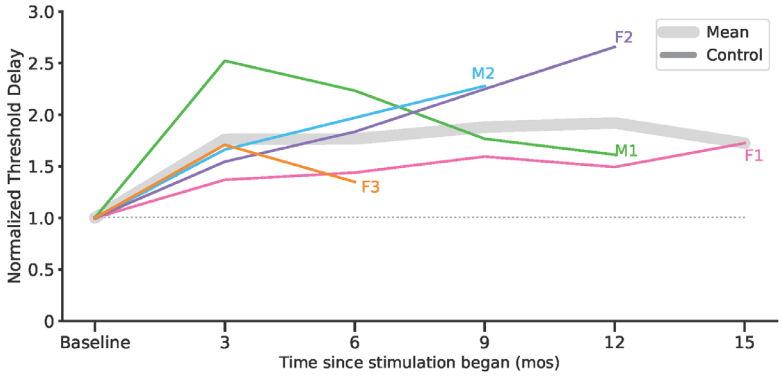

Figure 2. Long-term changes in the five animals from Figure 1D. The three month time period includes the data from Figure 1D, while the other time points include data from 1F and after in which variable stimulation protocols were followed as detailed in Figure S4.

The treatment of dementia often utilizes cholinesterase inhibitors, which prolong the action of acetylcholine by inhibiting its hydrolysis. The most commonly prescribed cholinesterase inhibitor is donepezil, and we have previously shown that it can acutely improve working memory in monkeys[9]. To assess whether it could also provide enduring improvement of working memory monkeys were given donepezil daily after their working memory tests. Monkey performance in the period before and after donepezil administration is shown in Figure 1G, for a cohort of six monkeys that did not receive stimulation implants. Grouping and normalizing the data as was performed for the stimulated animals did not result in a significant difference between groups ($F(1,4)=0.66$, $p=0.46$).

A further positive stimulation control treatment consisted of electrodes that were not placed in the subpallidal basal forebrain and were stimulated with the same parameters as the treatment group. As shown in Figure S2, this treatment did not result in a consistent improvement in working memory duration. Electrode misplacement by more than 2 mm from the desired targets occurred in either the mediolateral or anterior posterior plane. For this group, the changes caused by stimulation were not significant ($F(1,2)=0.4$, $p=0.59$).

To understand the nature of behavioral improvement and whether stimulation produced a bias we examined sessions with unilateral stimulation. This seemed unlikely from the outset since the stimulus to be remembered was always presented in the center of the screen and two choices followed it, making it unlikely that monkeys would be biased to erroneously select the stimulus contralateral to stimulation. In fact, stimulation tended to reduce preexisting biases, that monkeys developed at baseline, as has been previously shown[25], in the form of modest preferences for correct targets on one side compared to the other (right vs left). One example is shown in Figure 3D. Stimulation reduced the bias, and this effect was significant in 2 of the 5 subjects ($p=0.0023$ and 0.0019), as shown in Figure 3D-E. The change in bias was predicted by the pre-study bias, shown in Figure 3E ($R^2 = 0.66$, slope = -0.56, $p = 0.03$; Monte Carlo 95% CI [-0.79, -0.31]). The results suggested that stimulation enhanced the memory representation in a fashion that allowed animals to correctly select the correct response, without having to resort to a default choice.

As prior work showed basal forebrain stimulation could acutely impair or improve working memory depending on the stimulation pattern in young monkeys[2–4], we evaluated acute stimulation effects in these elderly monkeys by comparing behavior while animals were normalized by their performance without stimulation. Notably, the pulse pattern used in this study applied 20 seconds of pulses interspersed with 40 second off periods, which had previously been shown to acutely improve performance in young male adults. As shown in Figure 3A, in the first four weeks, stimulation during task performance impaired behavior compared to task performance without stimulation (t-test on adaptive tracking reversals pooled across monkeys, $t(504)=5.90$ $p<10^{-8}$). The mean behavioral thresholds during stimulation were only 70% as long as the thresholds without stimulation in this first four week period. However, by the last four week period, the adaptive tracking threshold

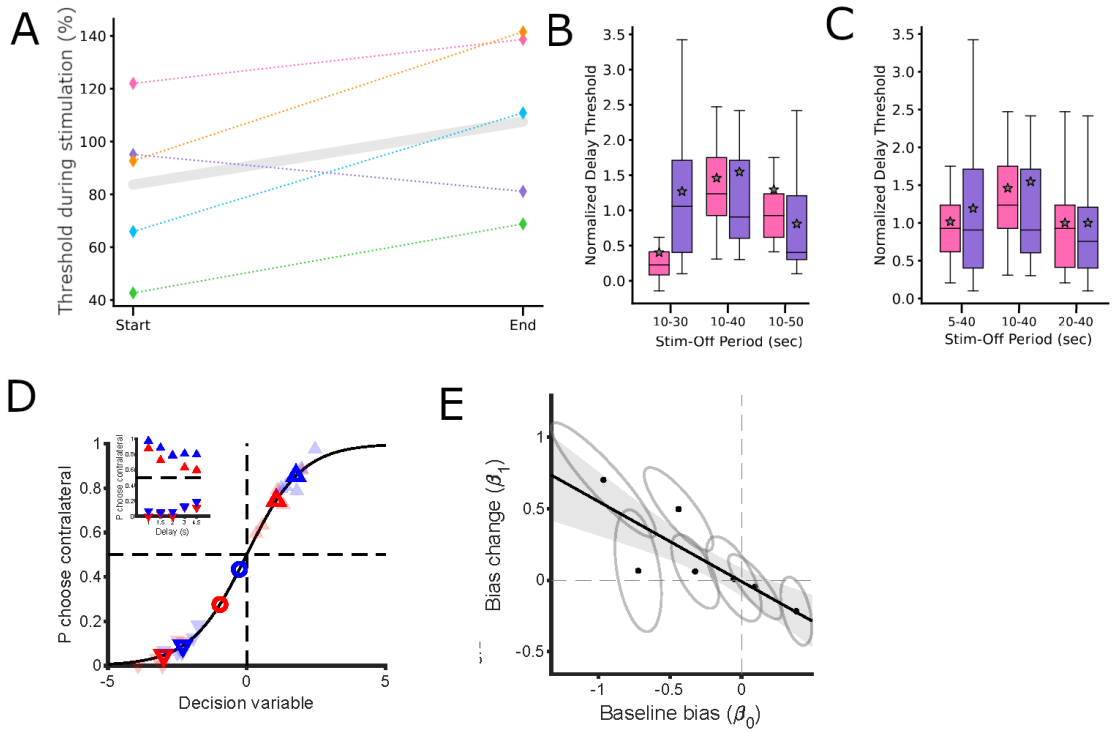

Figure 3. A. Acute effects of stimulation. Each line shows data from one animal, and the thick gray line shows the population mean. Data are threshold during stimulation as a percentage of threshold without stimulation. B and C. Threshold for animals F1 and F2 under different bilateral stimulation and recovery period conditions. Performance thresholds were maximized using 10 seconds ON, and 40 seconds OFF, which outperformed other tested patterns. D. Logistic fit of an example animal's choice patterns pre- and post-treatment. Upward and downward hollow triangles represent the delay averaged choice probabilities to the cue contralateral to the stimulation electrode when that cue matched and did not match the sample respectively. The circles represent the bias. Red and blue markers represent the pre- and post-treatment performance respectively. Solid triangles indicate the choice probabilities at each delay. E. The amount of bias correction was predicted by the baseline bias level. Ellipses indicate the 95% confidence interval. Shaded area represents the simulated 95% prediction.

during or in the absence of stimulation were nearly matched. When thresholds during stimulation were normalized by monkey and time period and pooled, the effect of stimulation on threshold in the first four weeks was significantly worse than the stimulation effect over the last four weeks (t-test on adaptive tracking reversals pooled across animals, $t(418)=6.78$ $p<10^{-10}$). The result suggests that benefits of stimulation for old monkeys emerged as a result of long-term plastic changes conferred by the stimulation, and did not require positive acute effects of concurrent stimulation during behavior.

Experiments described so far relied on the same stimulation parameters, involving 20 seconds of stimulation followed by 40 of no stimulation. We wished to explore more the parameter space that optimizes the behavioral benefit. Therefore, stimulation was next evaluated by using parameters that included a different balance of stimulation and recovery. The acute impairment in working memory during stimulation in these aged macaques contrasts with the acute improvement in younger animals[9]. Recent mouse imaging work also suggested that the stimulation period was too long, and the recovery period too short, to achieve maximal acetylcholine bursts in each cycle[10]. Two animals were thus stimulated bilaterally with different parameters. As shown in Figure 3B-

C and S3, working memory performance was tuned to the stimulation parameters of a 10 second ON period and a 40 second OFF period (10-40) in these two animals. These parameters bested parameters with shorter or longer ON or OFF periods, and resulted in a 40% increase in working memory duration threshold compared to 20-40. The data were pooled across monkeys to show that there were significant effects of recovery period when the stimulation period was 10 seconds ($F(2)=6.4$, $p<0.02$), and that there were significant effects of stimulation period when the recovery period was 40 seconds ($F(2)=7.4$, $p<0.03$). In post-hoc testing, the 10-40 parameters resulted in significantly longer delays than the other groups in Figure 3B except the 10-30 group (Tukey HSD, all others $p<0.05$). The complete series of parameters evaluated are shown in Figure S3 in chronological order.

Finally, we investigated the underlying mechanisms through which stimulation improved cognitive performance. For this purpose, brain glucose utilization was also evaluated in three animals for whom we performed 18-F FDG-PET imaging before and after twelve weeks of stimulation. Glucose utilization is a marker that consistently tracks progression of Alzheimer's dementia[20,21]. Animals received one hour of daily intermittent stimulation, and the effect of stimulation on the standardized uptake value ratio relative to the ipsilateral pons (SUVr-pons) was compared on the stimulated side, with the unstimulated side as control. Statistical maps were thresholded to find large enough clusters of suprathreshold voxels. Stimulated hemispheres had three significant patches of increased glucose utilization relative to the unstimulated hemisphere (all $t(8)>3.355$, $p<0.005$, see Methods), with no clusters of decreased utilization, shown in Figure 4A. Without stimulation larger clusters showed decreased glucose utilization making up 18% of the hemisphere, with no clusters of increased utilization. Using standard atlas parcellation, we also compared glucose utilization by region in these three animals, and the regions strongly trended to have higher utilization (40 of 51 comparisons positive, $p = 5.70E-5$, binomial test) on the stimulated hemisphere as shown in Figure 4B.

We also measured whether activation of neurotrophic pathways was occurring in our preparation. Rodent work has indicated that expression of the receptors for the neurotrophins nerve growth factor (NGF) and brain derived neurotrophic factor (BDNF) are increased by this stimulation[10], which suggests that the neurotrophins are being released and/or activated. This release is hypothesized to occur into the interstitial fluid of the cerebral cortex, which slowly mixes with cerebrospinal fluid[22,23]. The fluid turns over in 6-8 hours, and mixes completely with cerebrospinal fluid (CSF) in less than half that time. In four of the monkeys, CSF was sampled before and after one hour of stimulation in the 20 ON-40 OFF condition. The fluid was tested for its concentration of tissue plasminogen activator (tPA), which is an activating element in the pathways for both NGF and BDNF. We found tPA levels in the same range as is documented in humans[24], and that the levels increased significantly and by two to three-fold by stimulation ($t(3)=3.59$,$p<0.04$), as shown in Figure 4C.

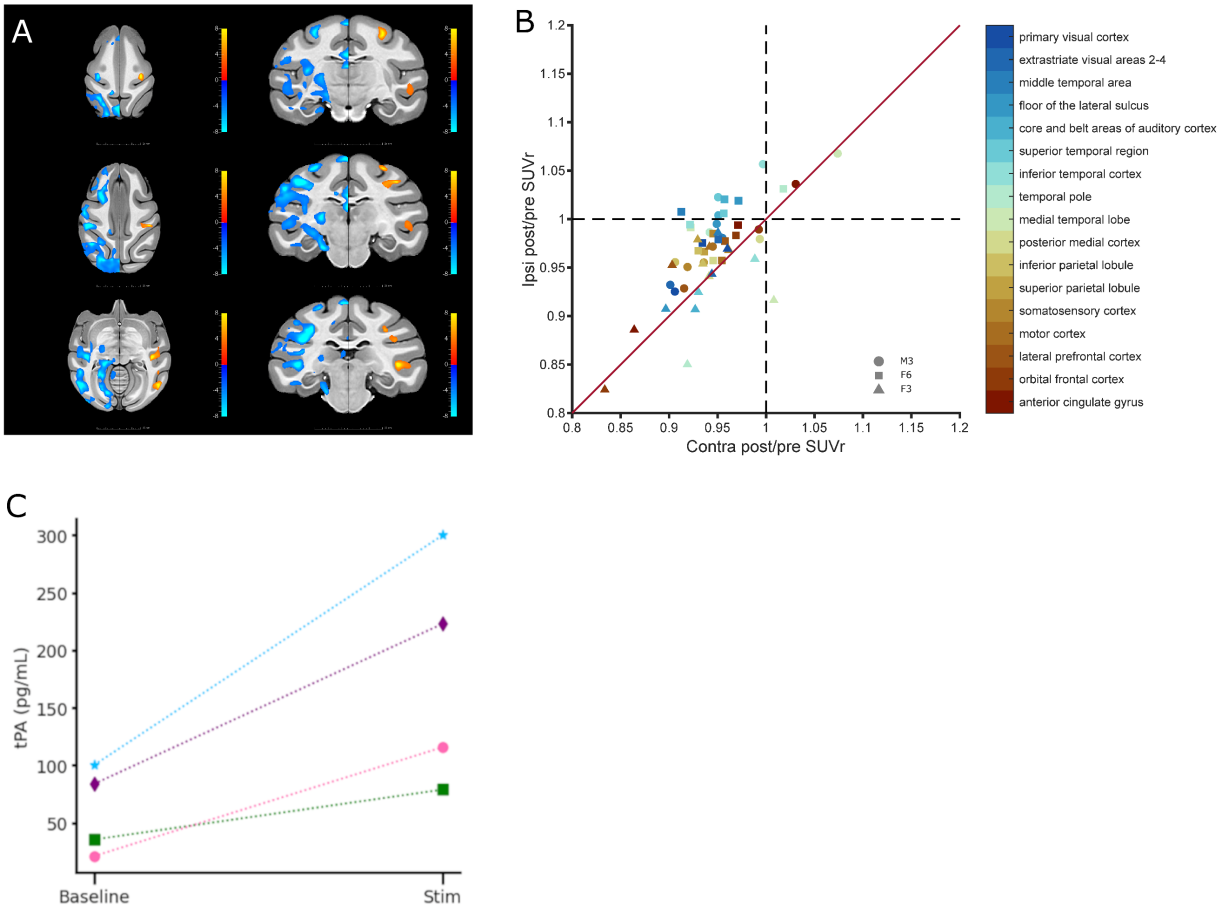

Figure 4. 4. A. Statistical maps of lateralized effects on 18-F PET-FDG SUVr-pons. Hemisphere on image left: significant clusters with time-dependent changes in glucose uptake. Hemisphere on image right: significant clusters with stimulation-dependent changes in glucose update, after controlling for time-related effects. B. Comparison of 12 week change ratios in PET SUVr between stimulated and unstimulated in 17 cortical regions. C. Tissue plasminogen activator was measured in cerebrospinal fluid under neutral conditions or after a one hour stimulation period in four animals.

Deep brain stimulation has been used extensively in the treatment of movement disorders, and increasingly for the treatment of depression, epilepsy and obsessive-compulsive disorder[26]. In most applications, continuous, 24 hour per day high frequency pulse trains are used to normalize the output of abnormally hyperactive circuits that receive the stimulation. Multiple hypotheses exist on the mechanisms that support this normalization[27]. In contrast, shorter pulse trains are used in animal models to activate cortical circuits[28–30], rather than to suppress them. We applied short pulse trains, with recovery periods, over one hour daily with intent on increasing the activity of the circuits. The increased NGF and BDNF receptor expression found from this stimulation in mice[10], along with the increased CSF concentration of tPA found in the present study, support the premise that this pattern of stimulation increases the forebrain cholinergic projection to enhance neurotrophic activity. The neurodegeneration of this forebrain region predicts non-motor executive function cognitive loss in Alzheimer's, Lewy Body and Parkinson's dementia[6,7,31,32], so its improved function from intermittent deep brain stimulation is a candidate for improving executive function in these populations.

We found that applying stimulation during behavior resulted in an acute impairment, while stimulation both during and after behavior resulted in long-term performance improvement. Over time, this acute impairment becomes neutral. Our prior work in young male monkeys found consistent improvement with the same parameters, 20 second pulse train at 60 Hz interspersed with 40 second rest periods[2–4]. Work in young and old

monkeys has found donepezil to acutely improve working memory[5]. These data, together, suggest that increases in cholinergic function lead to improved working memory, and the neural basis of this improvement has been explored[4,6]. Together, these data suggest that the acute impact of intermittent stimulation using parameters defined from young male monkeys result in different neuromodulation in elderly animals. The tuning of the parameters for optimizing long-term improvements in working memory further discovered that half as much stimulation per cycle, 10 seconds instead of 20, resulted in 40% longer working memory duration. This remains the most plausible hypothesis for the difference in this study and prior work, that elderly animals require a different balance of stimulation and rest to optimize acute effects.

As intended, the stimulation perfuses the cerebral cortex with acetylcholine, with a recovery period, prior to perfusing the cerebral cortex again. Cholinergic activation has previously been shown to cause the release of neurotrophins and tissue plasminogen activator[2,33], which are our leading hypotheses for key elements leading to improved behavioral function. The neurotrophins are necessary for multiple forms of synaptic and map plasticity in the cerebral cortex[34–36], and in the nonhuman primate preparation tPA and neurotrophins may be readily measured by their concentrations in CSF. The creation of NGF by stimulation should elaborate the arborization of cholinergic axons into the cerebral cortex, and result in greater acetylcholine release[37]. BDNF, in turn, has effects that include increased coupling between parvalbumin interneurons and pyramidal neurons[38].

The potential application of this form of stimulation to improve cognition, especially in dementia, is also beginning to be explored. Three Parkinson's patients, receiving this pattern of stimulation for two weeks, improved in their sustained attention, compared either to baseline, or to performance after two weeks of 20 pulse per second continuous stimulation[11]. Deep brain stimulation to reduce activity in neural circuits has been heavily explored for the past two decades; today, we begin to explore the potential of deep brain stimulation to increase activity in neural circuits.

Acknowledgments

Work on this supported by NIH/NIA grant RF1AG060754 and by a public/private partnership agreement between Boston Scientific and the institutions of the investigators CC and DTB. Boston Scientific provided Spectral Wavewriter implantable pulse generators, controller tablets, and connecting hardware, as well as scientific expertise from M. Moffitt and W. Gu. We would like to thank K. Shanazz and R. Jagirdar for their histological help in localizing electrolytic lesions, C. Suell, K. Clemencich, K. Yetman, M. Plagenhoef and J. Sun for technical help with animal testing and surgeries and C. Cryan for work in the first ELISA tests of CSF for tPA.

Bibliography **(limited to 50)**

1. Sato, A. & Sato, Y. Cholinergic neural regulation of regional cerebral blood flow. *Alzheimer Assoc Disord* **9**, 28–38 (1995).
2. Hotta, H., Kagitani, F., Kondo, M. & Uchida, S. Basal forebrain stimulation induces NGF secretion in ipsilateral parietal cortex via nicotinic receptor activation in adult, but not aged rats. *Neurosci. Res.* **63**, 122–128 (2009).
3. Coyle, J., Price, D. & DeLong, M. Alzheimer's disease: a disorder of cortical cholinergic innervation. *Science* **219**, 1184–1190 (1983).
4. Sarter, M. & Bruno, J. P. Cognitive functions of cortical acetylcholine: toward a unifying hypothesis. *Brain Res. Rev.* **23**, 28–46 (1997).
5. Terry Jr., A. V. & Buccafusco, J. J. The cholinergic hypothesis of age and Alzheimer's disease-related cognitive deficits: recent challenges and their implications for novel drug development. *J Pharmacol Exp Ther* **306**, 821–827 (2003).
6. Grothe, M. J. *et al.* Atrophy of the cholinergic basal forebrain in dementia with Lewy bodies and Alzheimer's disease dementia. *J. Neurol.* **261**, 1939–1948 (2014).
7. Crockett, R. A., Wilkins, K. B., Aditham, S. & Brontë-Stewart, H. M. No laughing white matter: Reduced integrity of the cortical cholinergic pathways in Parkinson's disease-related cognitive impairment. *Neurobiol. Dis.* **185**, 106243 (2023).
8. Mesulam, M. M., Hersh, L. B., Mash, D. C. & Geula, C. Differential cholinergic innervation within functional subdivisions of the human cerebral cortex: a choline acetyltransferase study. *J. Comp. Neurol.* **318**, 316–28 (1992).
9. Liu, R. *et al.* Intermittent Stimulation of the Nucleus Basalis of Meynert Improves Working Memory in Adult Monkeys. *Curr. Biol.* **27**, 2640–2646 (2017).
10. Kumro, J. *et al.* Chronic basal forebrain activation improves spatial memory, boosts neurotrophin receptor expression, and lowers BACE1 and Aβ42 levels in the cerebral cortex in mice. *Cereb. Cortex* bhad066 (2023) doi:10.1093/cercor/bhad066.
11. Sasikumar, S. *et al.* Rethinking NBM DBS: Intermittent stimulation improves sustained attention in Parkinson's disease. *Brain Stimul. Basic Transl. Clin. Res. Neuromodulation* **0**, (2023).
12. Kuhn, J. *et al.* Deep brain stimulation of the nucleus basalis of Meynert in Alzheimer's dementia. *Mol Psych* **20**, 353–360 (2015).

13. Sasikumar, S. *et al.* Single-Trajectory Multiple-Target Deep Brain Stimulation for Parkinsonian Mobility and Cognition. *Mov. Disord.* (2021) doi:10.1002/mds.28870.

14. Gratwicke, J. *et al.* Bilateral nucleus basalis of Meynert deep brain stimulation for dementia with Lewy bodies: A randomised clinical trial. *Brain Stimulat.* (2020) doi:10.1016/j.brs.2020.04.010.

15. Rattay, F. Analysis of Models for Extracellular Fiber Stimulation. *IEEE Trans. Biomed. Eng.* **36**, 676–682 (1989).

16. McIntyre, C. C., Grill, W. M., Sherman, D. L. & Thakor, N. V. Cellular Effects of Deep Brain Stimulation : Model-Based Analysis of Activation and Inhibition. *J. Neurophysiol.* **91**, 1457–1469 (2004).

17. Colman, R. J. Non-human primates as a model for aging. *Biochim. Biophys. Acta BBA - Mol. Basis Dis.* **1864**, 2733–2741 (2018).

18. Heuer, E., F. Rosen, R., Cintron, A. & C. Walker, L. Nonhuman Primate Models of Alzheimer-Like Cerebral Proteopathy. *Curr. Pharm. Des.* **18**, 1159–1169 (2012).

19. Levitt, H. Transformed Up-Down Methods in Psychoacoustics. *J. Acoust. Soc. Am.* **49**, 467–477 (2005).

20. Mosconi, L. *et al.* FDG-PET changes in brain glucose metabolism from normal cognition to pathologically verified Alzheimer's disease. *Eur. J. Nucl. Med. Mol. Imaging* **36**, 811–822 (2009).

21. Chételat, G. *et al.* Amyloid-PET and 18F-FDG-PET in the diagnostic investigation of Alzheimer's disease and other dementias. *Lancet Neurol.* **19**, 951–962 (2020).

22. Strecker, E. P. & James, A. E. The evaluation of cerebrospinal fluid flow and absorption: clinical and experimental studies. *Neuroradiology* **6**, 200–205 (1973).

23. Nedergaard, M. & Goldman, S. A. Glymphatic failure as a final common pathway to dementia. *Science* **370**, 50–56 (2020).

24. Pentz, R., Iulita, M. F., Ducatenzeiler, A., Bennett, D. A. & Cuello, A. C. The human brain NGF metabolic pathway is impaired in the pre-clinical and clinical continuum of Alzheimers disease. *Mol. Psychiatry* **26**, 6023–6037 (2021).

25. Terry, A. V., Jr., Jackson, W. J. & Buccafusco, J. J. Effects of Concomitant Cholinergic and Adrenergic Stimulation on Learning and Memory Performance by Young and Aged Monkeys. *Cereb. Cortex* **3**, 304–312 (1993).

26. Cagnan, H., Denison, T., McIntyre, C. & Brown, P. Emerging technologies for improved deep brain stimulation. *Nat. Biotechnol.* **37**, 1024–1033 (2019).

27. McIntyre, C. C., Savasta, M., Walter, B. L. & Vitek, J. L. How Does Deep Brain Stimulation Work? Present Understanding and Future Questions. *J. Clin. Neurophysiol.* **21**, 40–50 (2004).

28. Andersen, P., Sundberg, S. H., Sveen, O. & Wigström, H. Specific long-lasting potentiation of synaptic transmission in hippocampal slices. *Nature* **266**, 736–737 (1977).

29. Capocchi, G., Zampolini, M. & Larson, J. Theta burst stimulation is optimal for induction of LTP at both apical and basal dendritic synapses on hippocampal CA1 neurons. *Brain Res.* **591**, 332–336 (1992).

30. Cole, E. J. *et al.* Stanford Accelerated Intelligent Neuromodulation Therapy for Treatment-Resistant Depression. *Am. J. Psychiatry* **177**, 716–726 (2020).

31. Grothe, M. *et al.* Reduction of basal forebrain cholinergic system parallels cognitive impairment in patients at high risk of developing alzheimer's disease. *Cereb. Cortex* **20**, 1685–1695 (2010).

32. Mesulam, M. M. Cholinergic circuitry of the human nucleus basalis and its fate in Alzheimer's disease. *J. Comp. Neurol.* **521**, 4124–4144 (2013).

33. Bruno, M. A. & Cuello, A. C. Activity-dependent release of precursor nerve growth factor, conversion to mature nerve growth factor, and its degradation by a protease cascade. *Proc. Natl. Acad. Sci.* **103**, 6735–6740 (2006).

34. Pang, P. T. *et al.* Cleavage of proBDNF by tPA/plasmin is essential for long-term hippocampal plasticity. *Science* **306**, 487–491 (2004).

35. Hensch, T. K. Critical period plasticity in local cortical circuits. *Nat. Rev. Neurosci.* **6**, 877–888 (2005).

36. Mataga, N., Mizuguchi, Y. & Hensch, T. K. Experience-Dependent Pruning of Dendritic Spines in Visual Cortex by Tissue Plasminogen Activator. *Neuron* **44**, 1031–1041 (2004).

37. Ginty, D. D. & Segal, R. A. Retrograde neurotrophin signaling: Trk-ing along the axon. *Curr. Opin. Neurobiol.* **12**, 268–274 (2002).

38. Willis, A., Pratt, J. A. & Morris, B. J. BDNF and JNK Signaling Modulate Cortical Interneuron and Perineuronal Net Development: Implications for Schizophrenia-Linked 16p11.2 Duplication Syndrome. *Schizophr. Bull.* **47**, 812–826 (2021).

Supplementary Figures

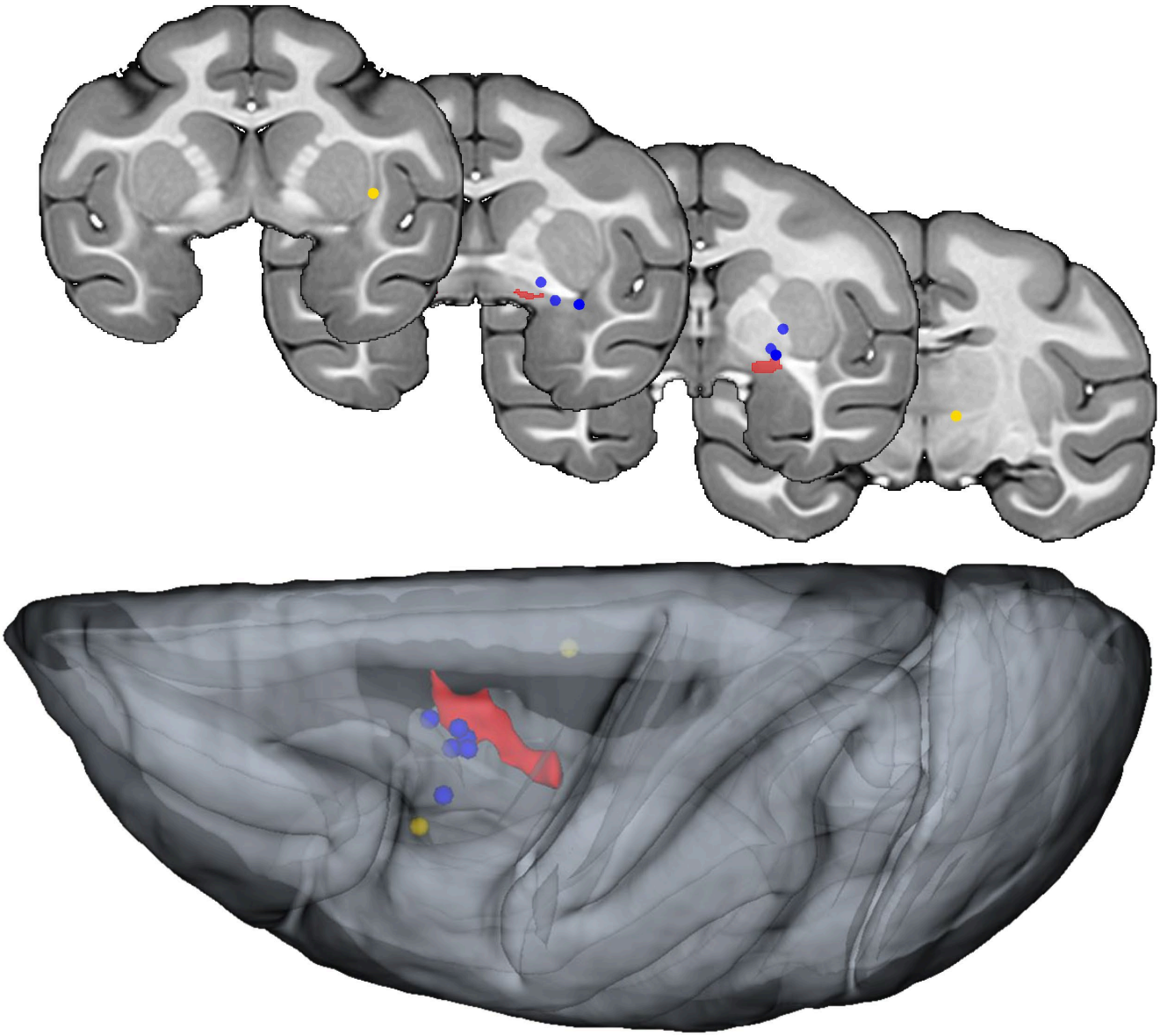

Figure S1. Electrode tip positions recovered by overlaying CT and MRI, or by electrolytic lesion localization. Blue indicates recovered positions considered in the inferior globus pallidus or nucleus basalis of Meynert/substantia innominata. Yellow indicates electrode tips that were not considered placed correctly for study. The red zone approximates the nucleus basalis of Meynert. All positions are mirrored into the same hemisphere for visualization.

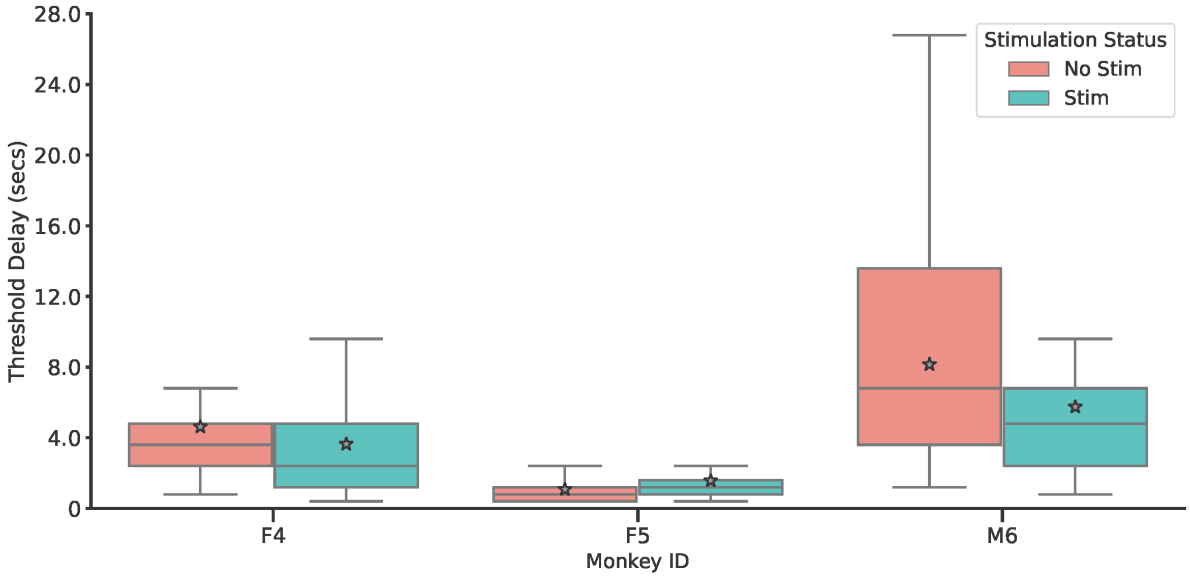

FigureS2. Boxplots of adaptive tracking reversal delays for three animals that received stimulation from electrodes not placed in or below the inferior globus pallidus.

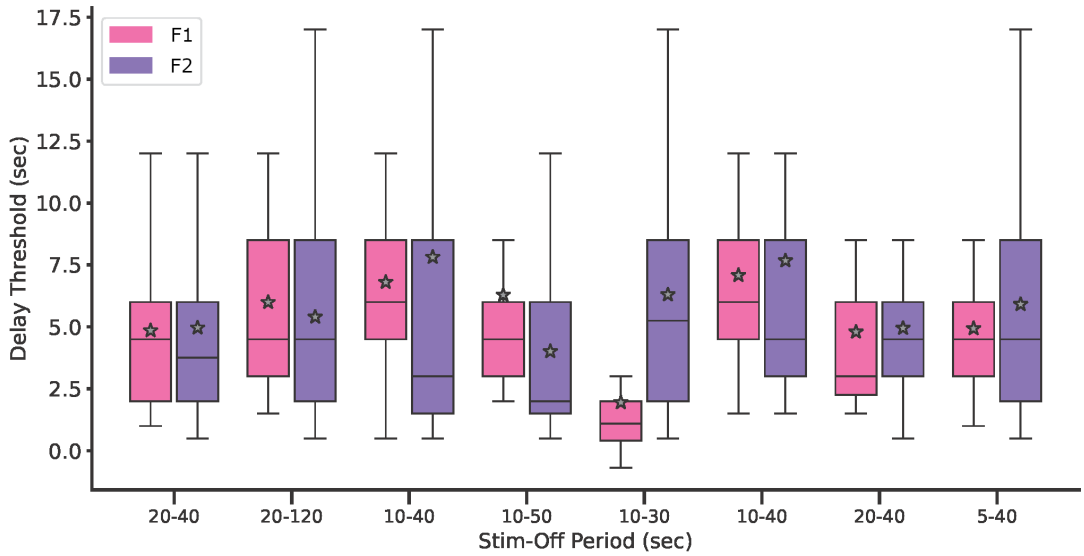

FigureS3. Boxplots of adaptive tracking reversal delays for two animals as a function of stimulation pattern. Data points from left to right were collected in chronological order. Four to five behavioral sessions were performed at each pattern.

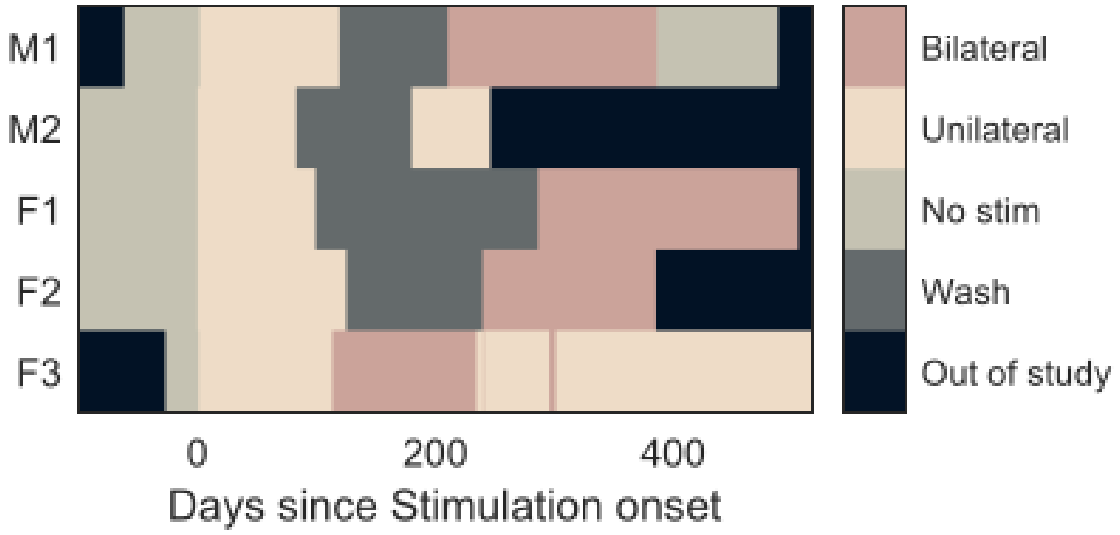

FigureS4. Stimulation history for animals in Figure 1D-F, and Figure 2. All animals received an 8-12 week period of unilateral stimulation beginning at day zero. Four had periods of at least 12 weeks without stimulation after the initial stimulation period. Three of the animals had bilateral working electrodes and received bilateral stimulation. Two of those are shown in Figure 3B-C.

Methods

Animals used in this study were 16 Rhesus monkeys Macaca Mulatta over 25 years in age. All had been used previously in behavioral pharmacology studies. Studies were performed at Augusta University and Vanderbilt University.

Surgical implantation

Surgeries were performed on isoflurane anesthesia. A methods paper describes these procedures in detail[1]. Animals were placed in a stereotaxic instrument using the ear canals and lower orbital ridges as fiduciary points. The Vanderbilt University animals had pre-operative MRI scans, and T1 images were used for planning targets. Augusta University used stereotaxic coordinates of 9 mm lateral, 19 mm anterior, and 29 mm deep from the lower surface of the bone. Similar coordinates were used at Vanderbilt except that the locations were corrected for altered alignment between the fiduciary points and the brain.

For the animals with imaging alignment, CT and MRI scans first were acquired. CT scans were acquired with a Philips (Amsterdam, Netherlands) Vereos PET/CT scanner, while MRI scans were acquired with a Philips 3T Ingenia Elition X scanner. MRI scans included a T1-weighted image with 0.5-mm isotropic voxels. The T1w image was skull-stripped and the brain parcellated into brain regions according to the symmetric NIMH Macaque Template (NMT) v2.0 of 0.25-mm isotropic voxels and the accompanying Cortical Hierarchy Atlas of the Rhesus Macaque (CHARM)[2] and Subcortical Atlas of the Rhesus Macaque (SARM)[3] using the @animal_warper function as part of the AFNI software[4]. This also generated a set of linear and nonlinear transforms that map the subject spaces from and to the template space. The CT and T1w images were aligned using the General Registration (BRAINS) module in 3D Slicer[5] which finds and applies a rigid-body transform. Alignment quality was manually verified. NB targets were identified from the atlas and visually confirmed/adjusted using the T1w image.

A Brainsight Vet system (Rogue Research Inc., Montréal, Canada) was used to plan the trajectory of implantation pre-surgically. The landscape of the skull surface was reconstructed from either the CT scan or the T1w image. The co-registration between the skull and the NB allowed the determination of the electrode's entry point and inserting angle.

The target was 2 mm posterior to the crossing of the globus pallidus by the anterior commissure, and in the floor of the globus pallidus. Bone screw holes 2-3 mm in diameter were drilled over the targets, and a bone screw with a hollow center (Gray-Matter Research, Bozeman MT) was installed. A guide cannula was inserted to point at the target. Electrodes were lowered into the cannula, the cannula was removed, and the electrodes were adjusted in depth. Silicone (Kwik-Sil, WPI Inc, Sarasota, FL, USA) was poured over the rear of the electrode to stabilize it in depth. After both electrodes were inserted, a wire connector from Boston Scientific, "a pigtail", was tunneled between the scalp and subscapular space. Individual pigtail wires were resistance welded to the uninsulated rear end of the electrode wire. The connectivity of each wire to the pigtail connector was then checked. The welds were potted in silicone, and the pigtail was silk-sutured to the galea to prevent slip. The skin was closed with inverted simple interrupted absorbable sutures. A pocket was opened in the subscapular space, and the implantable pulse generator (Spectra Wavewriter IPG, Boston Scientific) was inserted. The IPG was not connected while welding was conducted. Thereafter, the IPG and pigtail were connected, and impedance was tested. Generally impedances under 8 kOhms were noted. The subscapular skin wound was closed as above.

Electrodes

Electrode manufacture is described as in our methods paper[1]. The electrode is a 0.003" diameter wire insulated with PFA (A&M Systems, Sequim, WA). The tip of the electrode is stripped for a distance of approximately 1 mm. The rear connector end of the electrode wire was stripped for a distance of about 5 mm and was threaded through a stainless steel hypodermic tube that in turn was threaded through a polyimide tube. The wire was glued into the tubing with cyanoacrylate so that the one mm uninsulated on the lead end of the wire protruded from the tubing.

Behavior

Monkeys were trained for appetitive food pellets. A touchscreen was enclosed in a metal enclosure that also included a computer and a pellet dispenser. The training apparatus was mounted on the cage. Custom software ran 96 behavioral trials per day. In the working memory task, three rectangles were outlined on the screen, one centered and high on the screen, and two lower squares to the left and right of each other. The top rectangle illuminated with one color. Upon being touched, the square returned to the background color. The three rectangles were background color during the delay period. After the delay ended, the two lower rectangles were illuminated with the cue color, and a distractor color, until the monkey's choice by touch. Successful trials triggered the release of a food pellet, and unsuccessful trials with a time-out. Three successful trials resulted in a longer delay period, approximately a 50% increase each time. One unsuccessful trial resulted in a decrease in trial length to the previous shorter trial length, which was roughly 33% shorter. This three-up, one-down adaptive tracking can be used to measure the 79% threshold by averaging an even number of trial reversals[6]. The reversals are trials in which upward adaptive tracking changes to downward tracking, or vice versa. All animals were started on short intervals, and tracked to their working range over the early trials. Only reversals after trial 30 were used, and as many reversals as possible were used provided an even number were available. Only sessions in which greater than 70 of the 96 daily trials were used, and animals were used for a behavioral assessment only if they completed 70 trials in the preponderance of the sessions used for that assessment. This cutoff was used to avoid biases based on the time of session, and because it would result in too few reversals for adequate rigor in analysis. The same task was used each day. The colors used were generally yellow, blue, and red, but in some cases if animals had very long thresholds, a color scheme with more similar colors, such as three shades of blue, were used to keep the trial lengths shorter. The same colors were used, per animal, for all data presented.

Donepezil administration

Donepezil (Sigma-Aldrich, St. Louis, MO) was administered after behavioral training each day at a dose of 100-200 μg/kg per day. The 200 μg/kg dose was used for each animal, but in some animals, motivation for the behavior was reduced presumably from appetitive interactions, and lower doses (but above 100) were used in those animals. The highest dose tolerable, up to 200, was always used. The donepezil was delivered in a date after each behavioral session.

Electrode locations in positive controls

The mediolateral center of the globus pallidus floor, 2 mm posterior to the crossing of the pallidus by the anterior commissure, was the target in implantation. This target was chosen to avoid stimulating three off-target white matter tracts, the optic nerve, the anterior commissure, and the internal capsule. In three of the animals, the electrodes missed their targets as confirmed by imaging or post-mortem examination. In two of the cases, the midline between the ear canals in the stereotaxic device was more than 5 mm lateralized relative to the brain midline. These three animals constitute the positive stimulation controls in Figure S2.

Stimulation

All stimulation was delivered by spinal cord stimulators (Spectra WaveWriter, Boston Scientific) programmed to deliver bipolar pulses and externally controlled by the programming device.

FDG-PET image acquisition and preprocessing

All PET procedures were performed at the Vanderbilt site. 3 animals in the treated group with 9.5 ± 2.7 kg average body weight were each imaged once prior to bilateral electrode implantation and once during or shortly after receiving unilateral NB stimulation (2nd scan 288 ± 69 days (M ± SD) after 1st scan, 85 ± 30 days after stimulation onset). The animal was anesthetized with ketamine (15 -20 mg/kg) for induction and isoflurane (1 - 5%) for maintenance. The animal received an intravenous injection of [^{18}F]Fluorodeoxyglucose (FDG) with an average total radiopharmaceutical dose of 173.5 ± 5.1 MBq, before 31 frames of positron emission tomography (PET) scans were acquired between 2 min and 161 min on average after tracer injection. PET scans with a voxel size of 1×1×1mm were acquired with a Philips Vereos PET/CT scanner.

PET scans were preprocessed using the “volreg” and “align” blocks of the afni_proc.py pipeline in AFNI. Each sequence was motion-corrected, aligned to the T1w image using a rigid-body transform and further mapped to the standard template space using the transforms generated by @animal_warper. The final mapping accuracy was verified visually.

Standard uptake values (SUV) were then computed for each frame using equation 3, where r_t is the radioactivity activity concentration (Bq/mL) of the image acquired at time t (s) since tracer injection, w is the animal’s body weight (g), d is the total injected radiopharmaceutical dose (Bq) and $T_{1/2}$ is the half-life (s) of FDG.

$$SUV(t) = \frac{wr_t}{d} 2^{\frac{t}{T_{1/2}}} \tag{3}$$

SUV values of frames taken between the 40th and 60th min[7] in each sequence were averaged across frames and then normalized to the mean SUV in the ipsilateral pons due to its low age-related changes[8] and its lack of cholinergic projections from the basal forebrain. Normalizing within each hemisphere controls for any potential lateralized differences in signal intensity not specific to brain tissue. This procedure generated the Standard uptake value ratios (SUVr) measure which served as the dependent variable in subsequent analyses.

PET SUVr data analysis

To study the impact of stimulation on SUVr in the ipsilateral hemisphere, we utilized a linear mixed-effect model using MATLAB function fitglme by including “treatment stage”, “stimulated side” and their interactions as fixed-effect terms along with “subject” as a random-effect intercept term (equation 4). The reference levels of “treatment stage” and “stimulated side” were the baseline period and the contralateral hemisphere respectively. Thus, a positive effect of stimulation on SUVr in the ipsilateral hemisphere would be indicated by a positive coefficient for the interaction term, while a negative coefficient for the main effect of “treatment stage” would indicate an age-dependent decrease in SUVr orthogonal to stimulation.

$$\text{SUVr} \sim \text{treatment stage} * \text{stimulated side} + (1|\text{subject}) \tag{4}$$

For voxel-wise analysis, this model was computed for each voxel, resulting in 12 observations for each voxel and thus degrees of freedom (8, 1) for each fixed effect. For an effect to be significant in a voxel, the voxel-level one-tailed alpha level was chosen to be 0.005 (equivalent to a 0.01 two-tailed test). To control for familywise Type I error rate[9], we first estimated the spatial noise autocorrelation function (ACF) from each unilaterally-masked, individual SUV timeseries using AFNI’s 3dFWHMx function which assumed a mixture of Gaussian and exponential functions. The anatomical correlation was removed by fitting the timeseries within each voxel with a set of 5 reference functions (constant, linear, quadratic, sine, and cosine) using the “-detrend” option. Geometric means of the ACF parameters from all individual timeseries make up the final population average ACF (equation 5) with respect the Euclidean distance between voxels r in units of mm. Then using AFNI’s 3dClustSim function, we simulated the null distribution where each voxel in the unilateral brain mask was only significant by chance due to noise with spatial correlation described by the population average ACF. A spatially connected (first nearest neighbor, using the “-NN 1” option) cluster of all positive or all negative significant voxels (using the “bi-sided” output) larger than 72.59 mm^3 (4646 voxels) in size was found to be less likely than 0.05 in the null distribution. For each fixed effect in the model, clusters larger than this threshold was considered significant. The regions encompassed by the significant clusters were manually identified by overlaying the clusters on the template along with the CHARM and SARM atlases in 3D Slicer. For surface visualization, the T values within significant clusters were projected to the white matter surface of the NMT v2.0 template by averaging between the white matter surface and the pia surface using AFNI’s 3dVol2Surf function. The output was rendered using SUMA[10].

$$ACF(r) = 0.95 * \exp\left(-{r^2}/{2 * 1.88^2}\right) + (1 - 0.95) * \exp\left(-{r}/{0.39}\right) \tag{5}$$

For ROIs-based analysis, we followed the brain parcellation by the 2nd level of the CHARM atlas which segments the neocortex into 17 regions. SUVr was averaged within each unilateral ROI ipsilateral and

contralateral to each subject's stimulation side respectively. An additional random intercept for ROIs were added to the GLMM to test for average changes across the whole neocortex.

Behavioral statistics

The statistical approach in Figure 1 used adaptive tracking reversals as the primary measure. A tracking reversal occurs when the adaptive tracking algorithm changes from upward tracking to downward tracking, or vice versa. After trial 30 (of 96), each tracking reversal was included. If the number of tracking reversals on any day was an odd number, the earliest tracking reversal that day was dropped to ensure that each downward tracking reversal had a paired upward tracking reversal. The average tracking reversal was then evaluated, and all reversals for a specific animal were normalized by the average in the Baseline condition The average of an even number of reversals using 3-up 1-down tracking is 79%[6]. Then, a one-way ANOVA was used to evaluate whether the primary effect was statistically significant at $p<0.05$. As the tracking reversals were in a geometric, rather than an arithmetic, progression, the logarithm of the reversals was taken prior to testing the ANOVA. Significant results were followed by a Tukey's honestly significant difference was applied with a multiple comparison correction for the number of animals rather than the number of possible comparisons. The posthoc test was applied to each animal's Stim or Donepezil data to compare to the Baseline data. For the time course comparisons in Figures 1E the data were normalized by Baseline average and logarithm transformed, and data for all animals were combined, prior to application of a oneway ANOVA and Tukey's HSD posthoc test.

The tissue plasminogen activator assay was AbCam ab108914. CSF samples were selected from lumbar puncture except for two animals implanted with Ommayas, in which case the CSF was sampled from the Ommaya (Medtronic CSF ventricular reservoir 24106a, neonatal sizing).

Mixed-effect logistic regression model for lateralization choice probability

Single-subject choice probability was modeled in a mixed-effect logistic regression model using MATLAB function fitglme. The design is specified in equation 1 where: Y_i was the binary response variable at delay i for which 1 indicated a response towards a contralateral cue that was inside the receptive field of the hemisphere primarily impacted by treatment (e.g., left cue when DBS was in the right NB), while 0 indicated a response towards an ipsilateral cue. t was the treatment stage, with the baseline period dummy coded as 0 and the first 12-week treatment period as 1. l was the laterality of the correct cue, with contralateral and ipsilateral cues dummy coded 1 and -1 respectively. Thus, β_0 was the log odds of bias in the baseline period; β_1 was the effect of treatment on bias; β_2 was the delay-average memory retrieval reliability and β_3 was the change in this reliability after treatment. b_{0i} was the random effect of delay on memory retrieval reliability, and b_{1i} was the random effect of delay on the treatment-based change in this reliability, allowing the estimation of the same fixed effects across delays. The random-effect coefficients were modeled to follow a zero-mean multivariate normal distribution specified in equation 2, where D was the covariance matrix between b_0 and b_1 which had 3 free parameters. The number of correct and total trials were aggregated across sessions by treatment stage, cue laterality and delay. Only delays at which at least 20 trials were completed under all 4 conditions (treatment stage × cue laterality) for all subjects were included, ensuring a balanced design for each subject and directly comparable β_2 and β_3 magnitudes across subjects.

$$\mathrm{logit}\big(P(Y_i = 1)\big) = \beta_0 + \beta_1 t + \beta_2 l + \beta_3 tl + b_{0i} l + b_{1i} tl \quad (1)$$

$$\boldsymbol{b} \sim N(0, D) \quad (2)$$

Mixed-effect model outputs from individual subjects were then pooled together to study the relationship between the pairs of parameters, namely the effect of treatment on bias (β_1) as a function of baseline bias (β_1) and the effect of treatment on memory reliability (β_2) as a function of baseline memory reliability (β_3). Linear regressions were carried out between each pair of model parameters. Since the distribution of each model parameter was given by the fitting, the uncertainty of these linear regression coefficients between model parameters can be additionally estimated by sampling from such distributions. Simulations were run by refitting the linear regressions on samples drawn from the posterior distribution of mixed-effect model parameters. Specifically, the mixed-effect model parameters from each subject followed a multivariate t-distribution

(sampled using MATLAB function mvtrnd), defined by the model parameter estimates, covariance matrix between parameters and degrees of freedom of error. The 95% confidence intervals were constructed from the 2.5th and 97.5th percentiles over 100,000 iterations of simulation.

Bibliography

1. Qi, X.-L. *et al.* Protocol for behavioral and neural recording during stimulation of the macaque monkey nucleus basalis. *STAR Protoc.* **3**, 101136 (2022).
2. Jung, B. *et al.* A comprehensive macaque fMRI pipeline and hierarchical atlas. *NeuroImage* **235**, 117997 (2021).
3. Hartig, R. *et al.* The Subcortical Atlas of the Rhesus Macaque (SARM) for neuroimaging. *NeuroImage* **235**, 117996 (2021).
4. Cox, R. W. AFNI: Software for Analysis and Visualization of Functional Magnetic Resonance Neuroimages. *Comput. Biomed. Res.* **29**, 162–173 (1996).
5. Kikinis, R., Pieper, S. D. & Vosburgh, K. G. 3D Slicer: A Platform for Subject-Specific Image Analysis, Visualization, and Clinical Support. in *Intraoperative Imaging and Image-Guided Therapy* (ed. Jolesz, F. A.) 277–289 (Springer, New York, NY, 2014). doi:10.1007/978-1-4614-7657-3_19.
6. Levitt, H. Transformed Up-Down Methods in Psychoacoustics. *J. Acoust. Soc. Am.* **49**, 467–477 (2005).
7. Jiang, Y. *et al.* Deep brain stimulation of the nucleus basalis of Meynert modulates hippocampal–frontoparietal networks in patients with advanced Alzheimer's disease. *Transl. Neurodegener.* **11**, 51 (2022).
8. Verger, A., Doyen, M., Campion, J. Y. & Guedj, E. The pons as reference region for intensity normalization in semi-quantitative analysis of brain 18FDG PET: application to metabolic changes related to ageing in conventional and digital control databases. *EJNMMI Res.* **11**, 31 (2021).
9. Eklund, A., Nichols, T. E. & Knutsson, H. Cluster failure: Why fMRI inferences for spatial extent have inflated false-positive rates. *Proc. Natl. Acad. Sci.* **113**, 7900–7905 (2016).
10. Saad, Z. S. & Reynolds, R. C. SUMA. *NeuroImage* **62**, 768–773 (2012).